General Disclaimer

One or more of the Following Statements may affect this Document

- This document has been reproduced from the best copy furnished by the organizational source. It is being released in the interest of making available as much information as possible.

- This document may contain data, which exceeds the sheet parameters. It was furnished in this condition by the organizational source and is the best copy available.

- This document may contain tone-on-tone or color graphs, charts and/or pictures, which have been reproduced in black and white.

- This document is paginated as submitted by the original source.

- Portions of this document are not fully legible due to the historical nature of some of the material. However, it is the best reproduction available from the original submission.

Battelle
Columbus Laboratories

Report

FINAL REPORT

on

MEASUREMENTS OF ELASTOHYDRODYNAMIC FILM THICKNESSES, WEAR, AND TEMPERING BEHAVIOR OF HIGH PRESSURE OXYGEN TURBOPUMP BEARINGS

(Contract NAS8-34908 Task 112)

to

NATIONAL AERONAUTICS AND SPACE ADMINISTRATION
GEORGE C. MARSHALL SPACE FLIGHT CENTER
Marshall Space Flight Center, Alabama

April 2, 1984

by

K. F. Dufrane, T. L. Merriman, J. W. Kannel,
R. D. Stockwell, D. Hauser, and J. A. Vanecho

BATTELLE
Columbus Laboratories
505 King Avenue
Columbus, Ohio 43201-2693

TABLE OF CONTENTS

LIST OF FIGURES

LIST OF TABLES

"MEASUREMENTS OF ELASTOHYDRODYNAMIC FILM THICKNESSES, WEAR, AND TEMPERING BEHAVIOR OF HIGH PRESSURE OXYGEN TURBOPUMP BEARINGS"

by

K. F. Dufrane, T. L. Merriman, J. W. Kannel,
R. D. Stockwell, D. Hauser, and J. A. Vanecho

INTRODUCTION

The reusable design of the Space Shuttle requires a target life of 7.5 hours for the turbopumps of the Space Shuttle main engine (SSME). This large increase from the few hundred seconds required in single-use rockets has caused various problems with the bearings of the turbopumps. The bearings of the high pressure oxygen turbopump (HPOTP) have been of particular concern because of wear, spalling, and cage failures at service time well below the required 7.5 hours. Battelle has been assisting NASA with these problems under a Task Order Agreement.

This particular Task was directed toward developing lubrication and wear data for the bearings. Since the HPOTP bearings operate in liquid oxygen, conventional liquid lubricants cannot be applied. Therefore, solid lubricant coatings and lubricant transfer from the polytetrafluorethylene (PTFE) cage have been the primary lubrication approaches for the bearings. Measurements were made in this Task using liquid nitrogen in a rolling disk machine to determine whether usable elastohydrodynamic films could be generated to assist in the bearing lubrication. Measurements were made of the wear rates of the AISI 440C bearing steel to assist in predicting the resulting ball wear if the solid lubricant films are consumed and not replenished. Measurements were also made of the tempering behavior of the AISI 440C to determine the effect of short heating cycles (from friction).

SUMMARY

The measurements of the elastohydrodynamic film thicknesses with liquid nitrogen under contact conditions simulating those of the HPOTP bearings have shown that the films are not sufficient to lubricate the bearing reliably. While measurable films are produced at reduced contact pressures, they are not sufficient to insure complete separation of the surfaces. There was also no indication of beneficial increases in the dynamic viscosity from the high pressures of the elastohydrodynamic contact. Therefore, lubrication of the HPOTP bearings must result from other approaches, such as solid-film coatings or transfer of solid films. The wear rates of AISI 440C steel in self-mated sliding contact without lubrication were found to be sufficiently high to explain the ball wear sometimes observed in the HPOTP bearings. The results confirm the need for lubrication for successful bearing operation. Hardness measurements on the AISI 440C with short tempering times showed that tempering times of 10 seconds or less can be tolerated at temperatures to 650 C (1200 F) without causing significant hardness reductions. A previously derived empirical relationship between hardness, tempering time and temperature was found to apply to the AISI 440C steel. It can be used to predict the hardness for various combinations of time and temperature. Measurements of hot hardness indicated that extended times at temperatures of 540 C (1000 F) are sufficient to reduce the hardness to unusable levels for bearing service. The results of the measurements underscore the critical need for reliable lubrication for the long-term success of the HPOTP bearings.

ELASTOHYDRODYNAMIC STUDIES WITH LIQUID NITROGEN

Experimental Apparatus

Disk Drive and Loading

The film thickness and traction measurements for the project were conducted with Battelle's twin-disk apparatus, shown pictorially in Figure 1, which was designed to study elastohydrodynamic (EHD) lubrication. The apparatus consists of two disks loaded against each other in rolling contact, each of which is driven by a variable frequency induction motor. The shafts of the drive motors are integral with the disk drive shafts and are mounted in duplex ABEC-4, 45 mm bearings. The electrical power to the motors is supplied by a variable-frequency supply unit. Disk speeds up to 15,000 rpm and continuously variable slip-ratios between the disks can be achieved.

Load is applied to the disk through a deadweight system with a mechanical advantage of 11.4 to 1. A pneumatic cylinder is used to support the load until it is desired in an experiment. This pneumatic arrangement also allows quick unloading of the disk when an experiment is completed.

In order to obtain disk contact pressures from a relatively low value of 170 MPa (25 ksi) up to the high pressure of 2100 MPa (300 ksi) experienced in the HPOTP bearings, the use of two sets of disks having different geometries was necessary. Descriptions of the two disk sets are given in Table 1. The 76 mm (3.0 in.) disks were used to produce the lower contact pressures and have the advantage of running at high surface velocities, as shown in Table 1. The intent was to perform film thickness measurements at speeds as close as possible to the surface speeds experienced in the SSME bearings, approximately 130 m/s (430 ft/s).

Load-stress curves are given in Figure 2 for the two disk designs. The 35 mm (1.4 in.) diameter disks were capable of producing the higher pressures because of the 140 mm (5.5 in.) crown on one of the

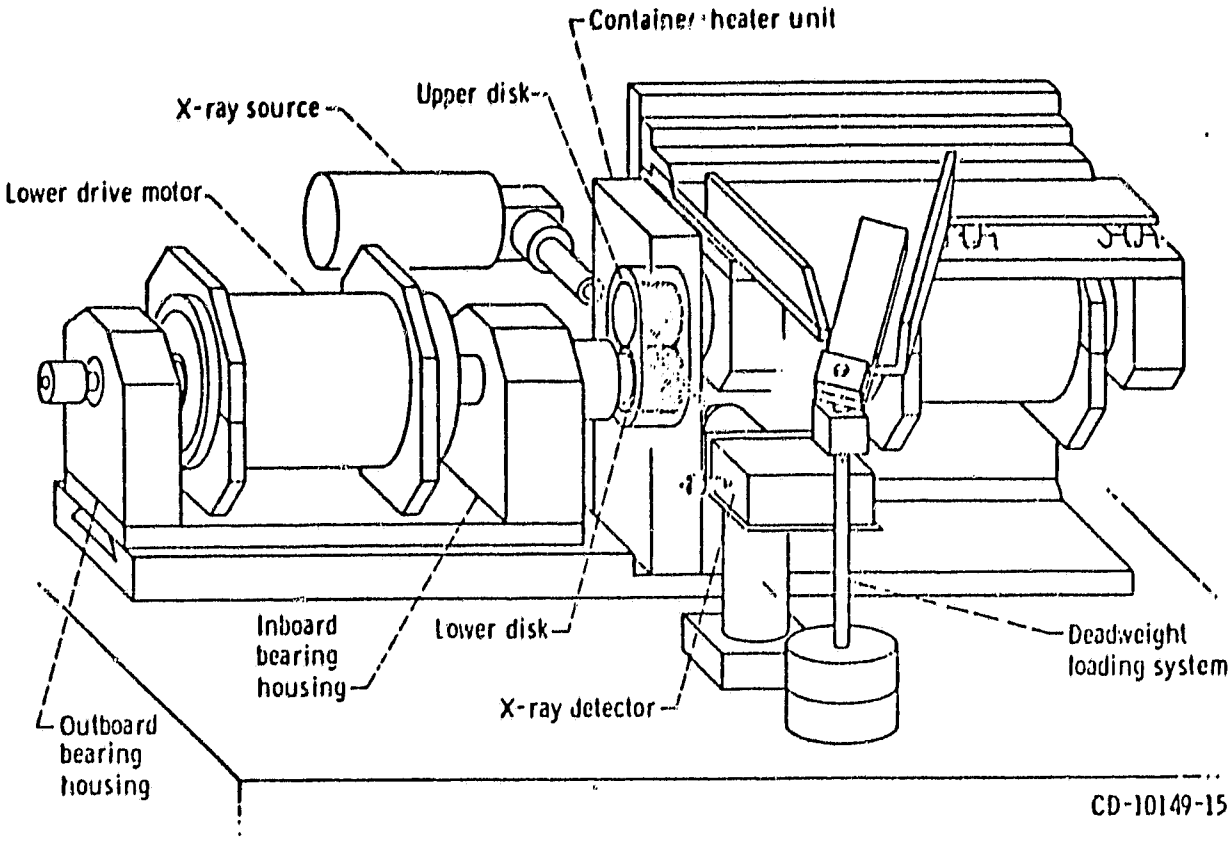

FIGURE 1. DISK APPARATUS USED IN EHD FILM THICKNESS EXPERIMENTS

TABLE 1. DISK PARAMETERS

Disk Set Outer Diameter(a), mm (in.)	Disk Material	Disk Surface Speed mm/s (in./s) at Shaft Speeds of		Average Surface Roughness of Disk Set mm x 10^{-6} (in. x 10^{-6})	
		5000 rpm	10,000 rpm	Before Test	After All Testing
76 (3.0)	Oildie Tool Steel	20,000 (790)	41,000 (1600)	<1	<3
36 (1.4)	M-50 Tool Steel	9400 (370)	19,000 (730)	<1	<2

(a) Upper disk of 36 mm (1.4 in.) diameter set was crowned with a radius of 140 mm (5.5 in.). All other disks of both sets were plain cylinders.

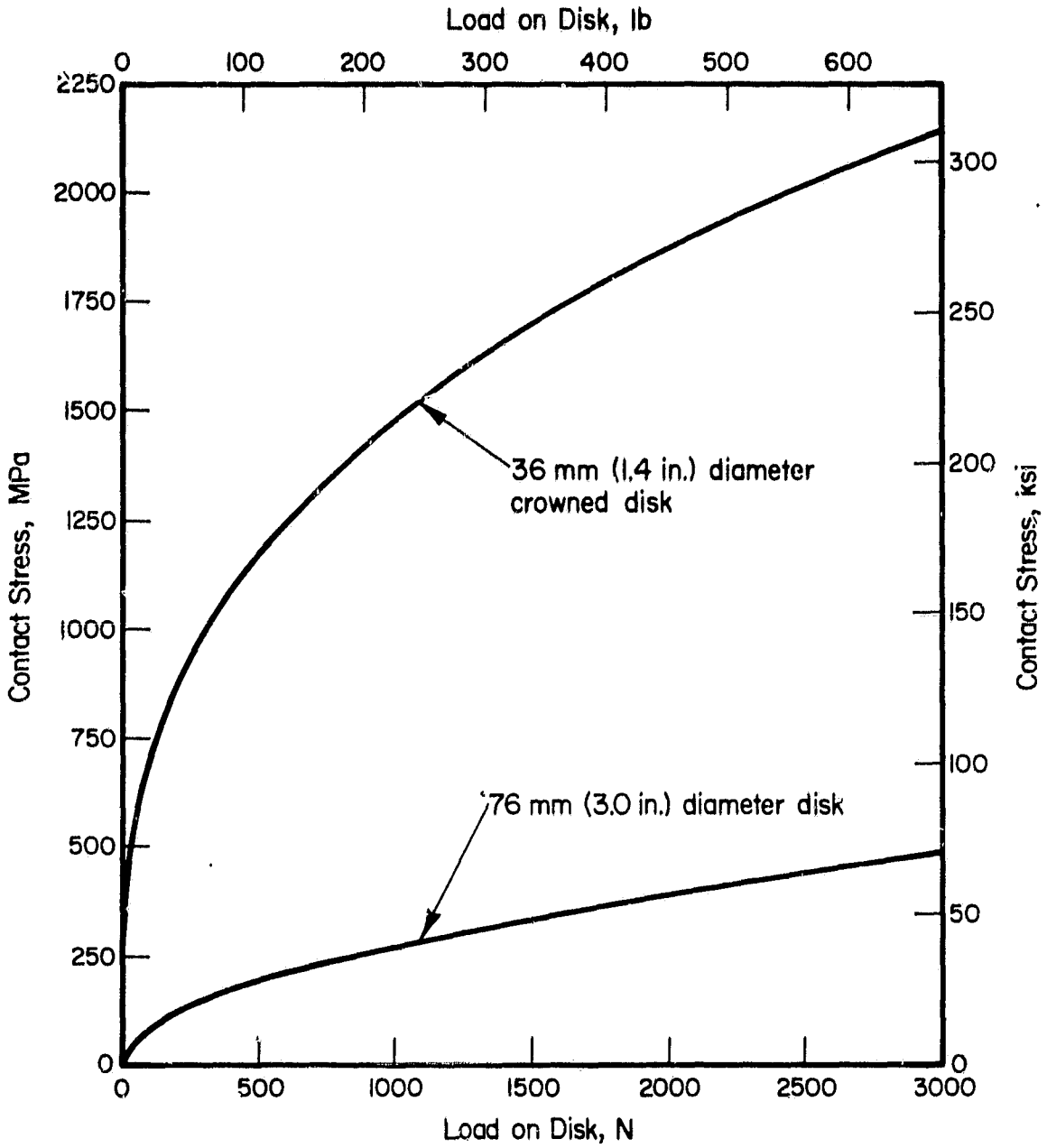

FIGURE 2. CONTACT STRESS AS A FUNCTION OF DISK LOAD

disks. The load-stress curves show the complete range of pressures which can be covered. A drawing of the 36 mm (1.4 in.) diameter disk set is given in Figure 3.

Film Thickness

The twin-disk apparatus has been used in numerous experiments involving conventional lubricants. For those experiments, lubricant is supplied to the disk through a pressurized jet directed at the disk contact region, which is supplied by a recirculating pumping system. For the cryogenic fluid studies of this project, liquid nitrogen (LN_2) was supplied to the disks on a once-through basis using tank pressure to deliver the fluid.

EHD film thicknesses between the rolling disk are measured by means of a collimated X-ray beam. X-rays pass readily through the fluid, but cannot pass through the opaque steel disks. By measuring the rate of X-ray transmission, the film thickness (gap) between the disks can be measured.

The twin-disk apparatus is also capable of verifying the film thickness measurements by measuring the electrical conductivity between the disks, which are electrically isolated. The method of isolation is shown in Figure 3. The continuity voltage is applied through a connection wire, shown in Figure 3, running from the outer portion of the upper disk, through the shaft center, to a slip ring. With a given applied external voltage, the actual voltage across the disks is a measure of the degree of separation by films generated between the disks. Since the conductivity of LN_2 is essentially zero (verified in tests during the study), decreased voltages are interpreted to be partial disk-to-disk contact.

Slip-Traction

The traction, or integrated shear stress in the film, is measured by changing the speed of the upper disk with respect to the lower

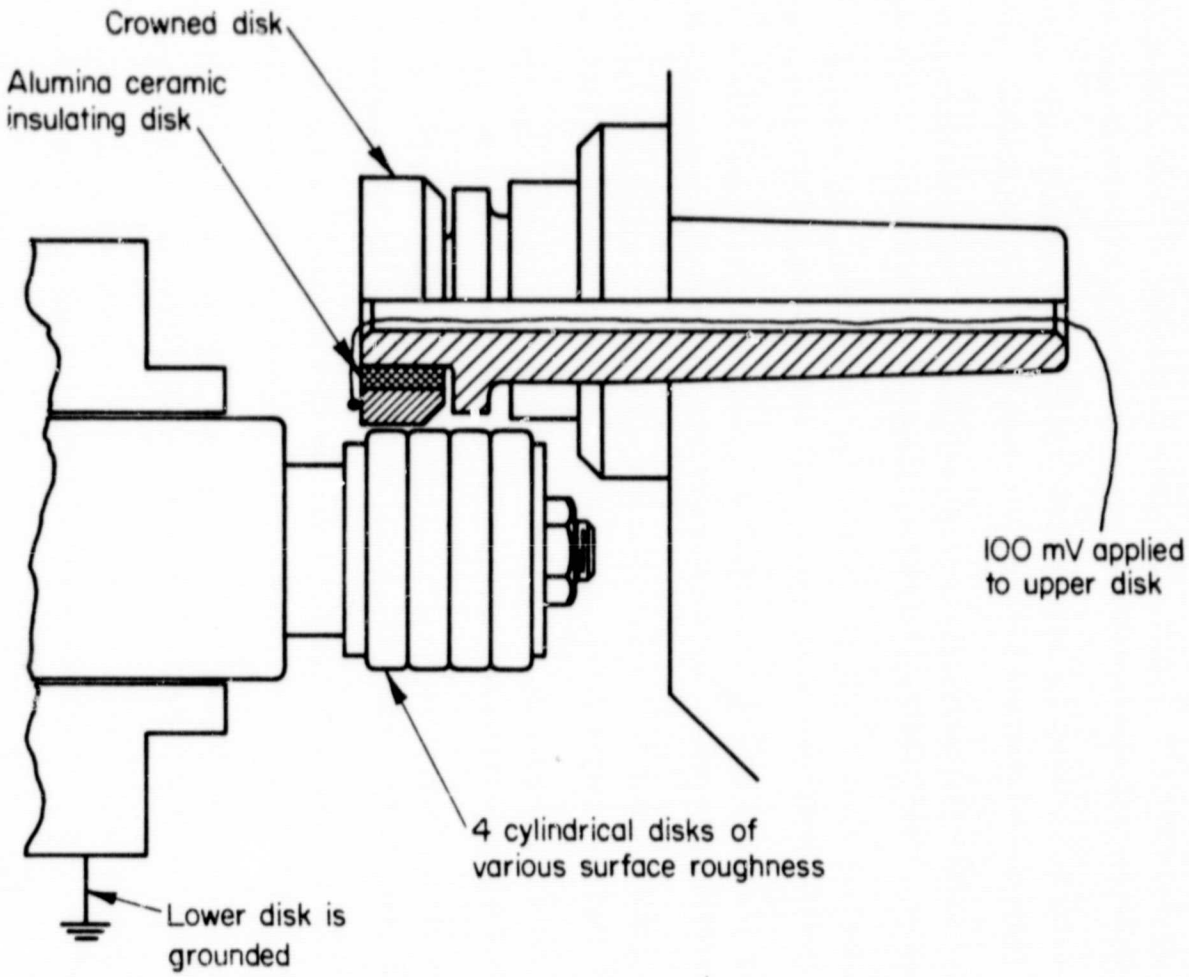

FIGURE 3. DETAILS OF 35mm (1.4 in.) DIAMETER DISK

disk and measuring the horizontal force required to restrain the upper motor assembly on which the upper disk is mounted. The upper motor is pivoted near the top and constrained with a load cell. The load cell output is calibrated with a standard weight while at running conditions. This calibration is checked prior to each series of tests.

Percent slip is defined as the speed differential between the upper and lower disk (x100) divided by the nominal speed. The lower disk is held at the nominal test speed (5000 or 10,000 rpm) while the upper disk speed is varied. Positive slip is defined as upper disk speed greater than lower disk speed. Percent slip is measured simultaneously with traction by a frequency-ratio meter. A digital storage oscilliscope records these two signals and plots traction-versus-percent slip.

For generation of the slip-traction curves, the slip was varied from at least a negative one percent to a positive five percent. Calculations based on the resulting data permit a calculation of the dynamic fluid viscosity within the EHD contact region.

Temperature Measurements

Five thermocouples were attached to the twin-disk apparatus in order to monitor temperatures during the tests. The thermocouples measured room temperature, the LN_2 reference temperature, the LN_2 jet outlet temperature, the temperature inside the test chamber, and the temperature of the lower disk.

EHD Film Thickness Measurements

Calibration and Check-Out

Several calibration and check-out procedures were performed prior to testing with LN_2. First the disks were axially aligned by traversing the X-ray beam across the disk and checking for a linear film thickness profile under mild operating conditions. This part of the procedure only applied to the cylindrical disks, since alignment is not

critical for a crowned disk profile. Before tests with the LN_2 were initiated, the accuracy of the film thickness measuring techniques were checked by running a film thickness experiment with a synthethic turbine oil, Mobil 2380 (MIL-L-23699-B), on which much previous work has been done.

Following the check-out experiments, the LN_2 flow was connected and the entire test chamber and disks allowed to equilibrate at LN_2 temperatures (-197 C). A positive pressure was maintained in the chamber from a gaesous nitrogen source to prevent the entrance of water vapor from the air. The disks were then statically loaded together and the intensity of the background X-ray radiation determined for each load. The disks were driven at the test speed (5000 or 10,000 rpm), the load applied, and the X-ray radiation through the film was measured. The film thickness was determined from the calibrated difference between the dynamic and static X-ray radiation levels.

While running at load, the temperature readings of the various points in the test chamber were monitored and recorded. The voltage across the electrically isolated disks was also recorded. Since the results with voltage levels of 1, 10, and 100 millivolts were generally found to agree, 100 millivolts was selected as a standard voltage to minimize the effects of electrica noise. From experience, the following correlation applies between the fluid film thickness and the voltage across the disks:

>75 to 100 mV = Full film lubrication

20 to 100 mV = EHD film breaking down, some surface asperities may touch

0 to 20 MV = No EHD film.

The film thickness and electrical conductivity data were recorded for increasing load conditions at each speed, until the film thickness fell below 0.25 μm (10 x 10^{-6} in.). This minimum film thickness was selected because the disks may be damaged if operated with thinner films.

Film Thickness Results

Measurements With 76 mm (3.0 in.) Diameter Disks. The LN_2 film thicknesses at the disk interface were recorded as a function of three variables in these experiments, namely: speed, temperature/inlet viscosity, and disk contact pressure. Disk temperature, however, was found to remain at -197 C; it never varied by more than two degrees. In order to average repeated data points and evaluate film thickness as a function of any one of the variables mentioned above, the data are customarily fit to an empirical equation where film thickness is a function of all three variables (speed, temperature/inlet viscosity, and contact pressure). For the case of LN_2 the temperature remained a constant and this eliminates variations in the inlet fluid viscosity. The particular equation chosen to fit the data was:

$$h = B\,(w)^{B2}\,(u)^{B3}\,(\mu)^{B4} \qquad (1)$$

or alternately,

$$\log(h) = B1 + B2\log(w) + B3\log(u) + B4\log(\mu) \qquad (2)$$

where

B = a constant

h = film thickness, μinches

w = contact pressure, ksi

u = disk speed, rpm

μ = fluid viscosity, at contact zone inlet, as a function of temperature

B1 = constant coefficient , log(B)

B2 = load coefficient

B3 = speed coefficient

B4 = viscosity coefficient.

This equation was chosen because previous investigators in elastohydrodynamic theory have derived this form from the Reynolds Equation and made comparison with empirical data[1, 2]*. These data were fit to Equation 2 by a linear regression program.

*References are listed on page 39.

All of the film thickness data for the 76 mm (3.0 in.) diameter disks are presented in Table 2. The accuracy of fit of the regressed data to the observed data is indicated by Figure 4. Agreement within 0.13 μm (5×10^{-6} in.) was considered to be a very good fit, and most of the data fall within these error bars. The film thickness data are presented graphically in Figure 5 for the 76 mm (3.0 in.) diameter disk at both shaft speeds.

The film thickness data at the lighter loads and higher speeds suggest that an adequate film is generated to separate the disks. However, the electrical continuity measurements indicate that the EHD film is not adequate (voltage < 75 mV) to separate the disks completely.

Measurements With 36 mm (1.4 in.) Diameter Disks. The 36 mm (1.4 in.) disks permit developing contact pressures up to those seen in the HPOTP bearings 2100 MPa (300 ksi). The results from all work with the 36 mm (1.4 in.) diameter disks are presented in Table 3. The conductivity and X-ray measurements both indicated very small films at all of the contact pressures studied. The X-ray film thickness measurements are not considered accurate for films less than 0.13 μm (5×10^{-6} in.), which is seen as the rather scattered film-thickness data reported. Therefore, the data were not regressed.

Another verification of very thin films was made by extrapolating the low pressure data to the higher pressures, with an adjustment being made for the different disk diameters. These data, presented in the last column of Table 3, show that the expected EHD film thicknesses are too thin to separate the disks at the high contact pressures.

Slip-Traction Measurements

Interpretation of Slip-Traction Curves

Additional information concerning the conditions in the high pressure contact region between disks can be gathered through the study

TABLE 2. FILM THICKNESS RESULTS WITH 76 mm (3.0 in.) DIAMETER DISKS

Contact Pressure, MPa (ksi)	Speed, rpm	Measured Voltage Across Disks, mV(a)	Film Thickness, μm (in. x 10^{-6}) Observed Data	Regressed Data
210 (30)	5000	12	0.64 (25)	0.69 (27)
210 (30)	5000	-	0.84 (33)	0.69 (27)
250 (35)	5000	15	0.46 (18)	0.48 (19)
250 (35)	5000	-	0.46 (18)	0.48 (19)
280 (40)	5000	15	0.25 (10)	0.36 (14)
280 (40)	5000	-	0.25 (10)	0.36 (14)
315 (45)	5000	7	0.25 (10)	0.28 (11)
315 (45)	5000	-	0.25 (10)	0.28 (11)
350 (50)	5000	4	0.30 (12)	0.20 (8)
350 (50)	5000	-	0.30 (12)	0.20 (8)
180 (25)	10000	30	1.80 (72)	1.5 (60)
180 (25)	10000	-	1.70 (68)	1.5 (60)
210 (30)	10000	28	0.97 (38)	1.0 (40)
250 (35)	10000	20	0.94 (37)	0.71 (28)
250 (35)	10000	-	0.64 (25)	0.71 (28)
280 (40)	10000	10	0.51 (20)	0.53 (21)
280 (40)	10000	-	0.51 (20)	0.53 (21)
320 (45)	10000	7	0.38 (15)	0.41 (16)
320 (45)	10000	-	0.25 (10)	0.41 (16)
350 (50)	10000	8	0.20 (8)	0.30 (12)
350 (50)	10000	-	0.33 (13)	0.30 (12)
390 (55)	10000	-	0.33 (13)	0.25 (10)
390 (55)	10000	-	0.33 (13)	0.25 (10)

(a) 100 mV applied across disks

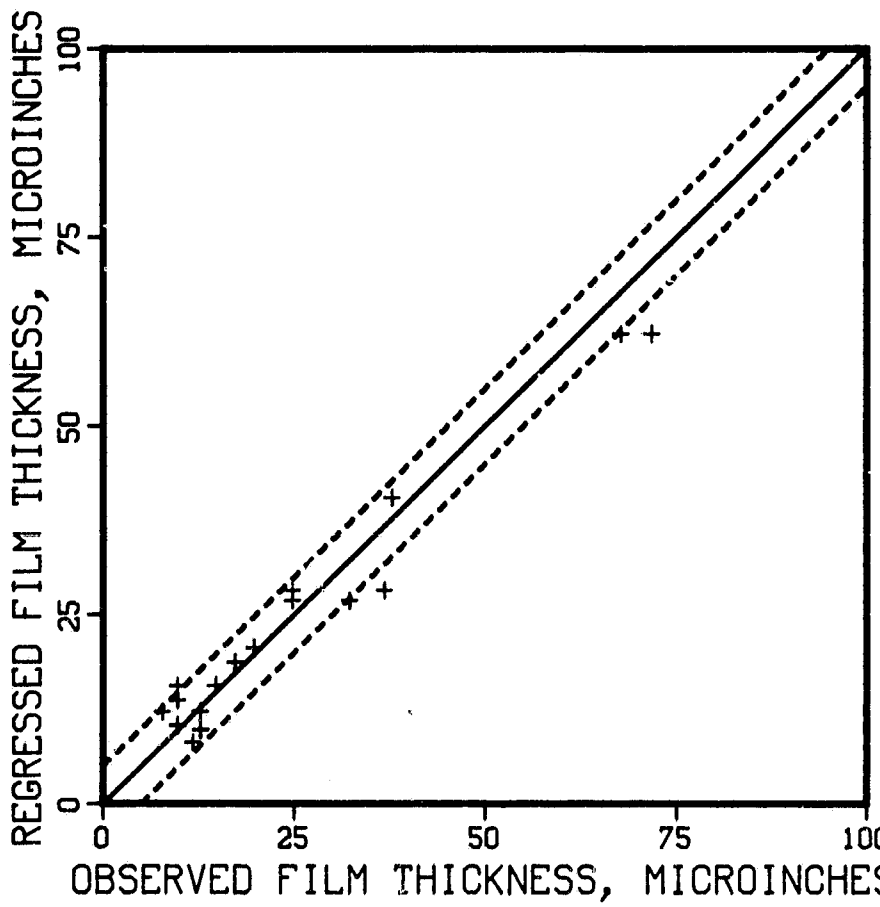

FIGURE 4. ACCURACY OF REGRESSION OF FILM THICKNESS DATA FOR 76 mm (3.0 in.) DIAMETER DISKS

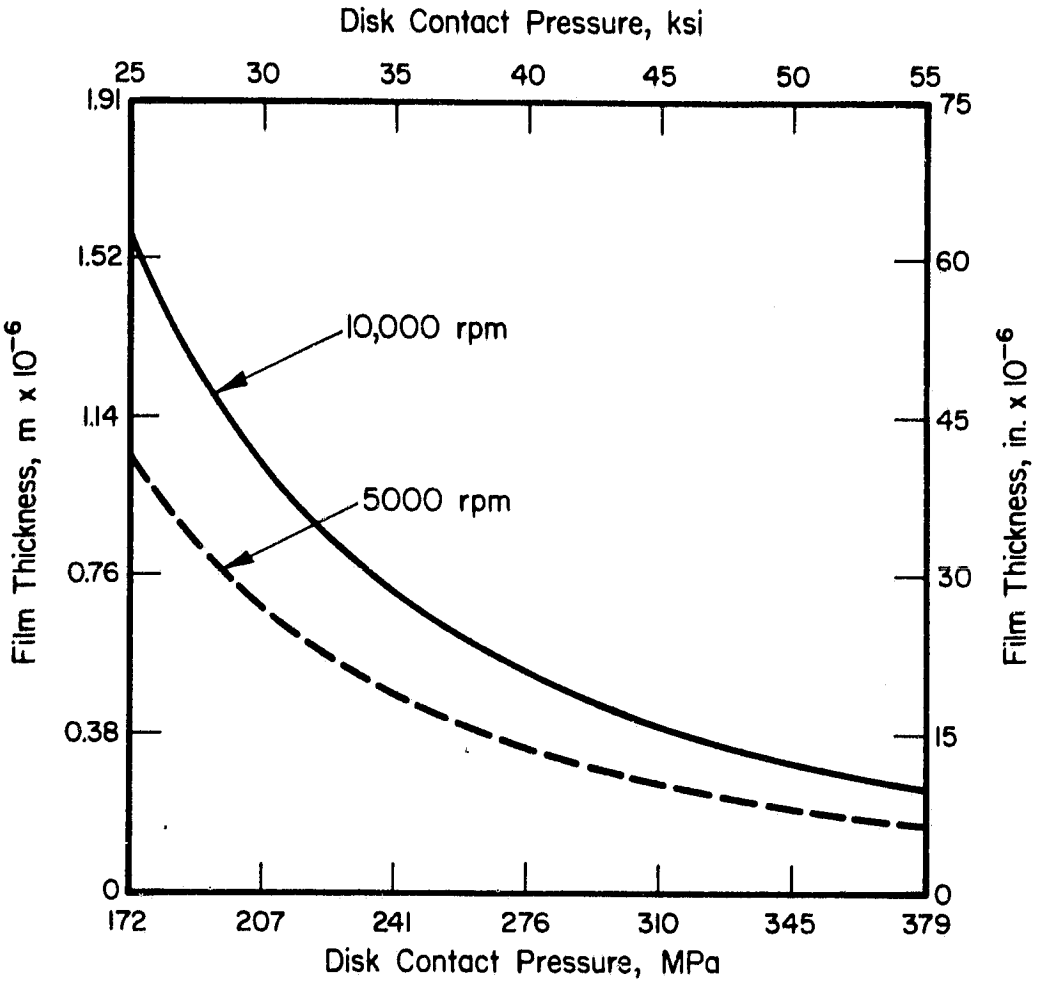

FIGURE 5. REGRESSED LIQUID NITROGEN FILM THICKNESS AS A FUNCTION OF LOAD CONDITIONS FOR 76mm (3.0 in.) DIAMETER DISKS

TABLE 3. FILM THICKNESS RESULTS WITH 36 mm (1.4 in.) DIAMETER DISKS

Contact Pressure, MPa (ksi)	Speed, rpm	Measured Voltage Across Disks, mV[a]	Film Thickness, μm (in. x 10^{-6})	
			Observed	Extrapolated from Lower Pressure
1000 (145)	5000	5	0.20 (8)	0.014 (0.54)
1000 (145)	5000	10	0.25 (10)	0.014 (0.54)
1200 (166)	5000	5	0.20 (8)	0.010 (0.39)
1200 (166)	5000	5	0.25 (10)	0.010 (0.39)
1300 (187)	5000	2	0.13 (5)	0.007 (0.29)
1300 (187)	5000	2	0.13 (5)	0.007 (0.29)
1000 (145)	10000	5	0.13 (5)	0.021 (0.81)
1000 (145)	10000	5	0.25 (10)	0.021 (0.81)
1200 (166)	10000	3	0.08 (3)	0.015 (0.59)
1200 (166)	10000	2	0.25 (10)	0.015 (0.59)
1300 (187)	10000	2	0.0 (0)	0.011 (0.44)
1300 (187)	10000	5	0.0 (0)	0.011 (0.44)

(a) 100 mV applied across disks

of the traction behavior of the fluid. If the disks are operating in an EHD regime where the disks are completely separated by the lubricant film, the slip-traction curve will reveal the shear characteristics of the lubricant. However, if the traction levels are much higher than expected for EHD films with the particular fluid under study, this indicates that the disk surfaces are in at least partial contact. Mixed film or boundary lubrication is therefore prevailing, and meaningful fluid viscosity data cannot be attained.

The method of analysis of a slip-traction curve is the same regardless of which lubrication regime is present. An example of a slip-traction curve is shown in Figure 6. Interpretation of the curve requires identifying the point of zero slip, which is the point of symmetry in the curve. Typically, this is located in the center of a region where traction varies linearly with slip. The slope of the slip-traction curve at the point of zero slip can be used to calculate the viscosity of the fluid at the particular contact pressure. If the assumption is made that a continuous fluid film separates the surface and the traction is produced by shearing a Newtonian fluid, the average shear stress ($\bar{\tau}$) can be calculated and related to the viscosity of the fluid at the average pressure in the contact. The traction (T) can be written as:

$$T = \bar{\tau} A = \mu \frac{\Delta u}{h} A \quad , \tag{3}$$

where

$\bar{\mu}$ = average viscosity at contact pressure

A = contact area between disks, as calculated from Hertzian Theory[1]

h = film thickness, as taken from the X-ray measurements

u = slip speed.

$T/\Delta u$ is the slope of the slip-traction curve as it passes through zero slip. With all other variables being known it is possible to solve for the average viscosity ($\bar{\mu}$) for a given pressure. A comparison of the results at a series of pressures determines whether the fluid is experiencing any pressure related changes in viscosity.

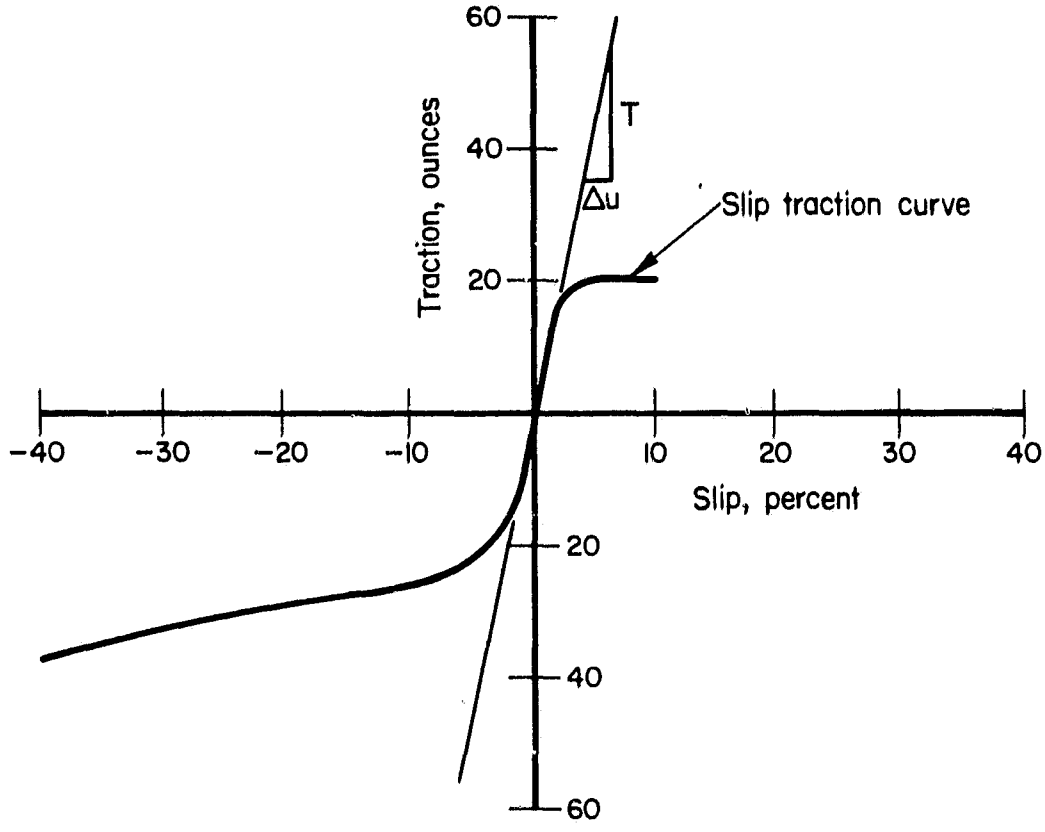

FIGURE 6. TYPICAL SLIP-TRACTION CURVE FOR CALCULATING DYNAMIC VISCOSITY

Results From LN_2 Slip-Traction Curves

Traction curves were taken for all of the conditions at which film thickness data were taken. Sample traction curves at two lower pressures, from 190 to 260 MPa (28 to 38 ksi), are presented in Figure 7 for a shaft speed of 5000 rpm and in Figure 8 at 10,000 rpm. The traction data further substantiated the electrical conductivity data of Table 3, which indicates very thin films. The traction levels were so high and erratic that it appeared the disks were approaching a dry rolling/sliding contact situation.

Average viscosity values at various pressures were calculated from the curves such as Figures 7 and 8 by the procedure described above, employing Equation (3). The results of these calculations are presented in Table 4.

The results show that there was not a significant viscosity change with pressure. The viscosities also appear much higher than would be expected, since the viscosity of LN_2 at atmospheric pressure is approximately 0.1 to 1 cp. Thus, the conclusion is drawn that the film, even at the lower pressures, was not sufficient to separate the disks completely. Therefore, the results in Table 4 do not represent valid viscosity data.

An interesting aspect of the experiments was the surface condition of both sets of disks after the complete series of experiments had been run. In past film thickness measurements with various types of fluids, the surfaces of the disks are likely to become roughened and require refinishing, if the disks are operated at film thicknesses less than 0.25 μm (10×10^{-6} in.). In the experiments with LN_2, however, even after operating a complete series of tests at high speeds and film thicknesses less than 0.25 μm (10×10^{-6} in.), the average surface roughness remained less than 0.08 μm (3×10^{-6} in.) R_A. This suggests that the cooling of the disks by the LN_2 is instrumental in preventing material transfer or scuffing between the disks.

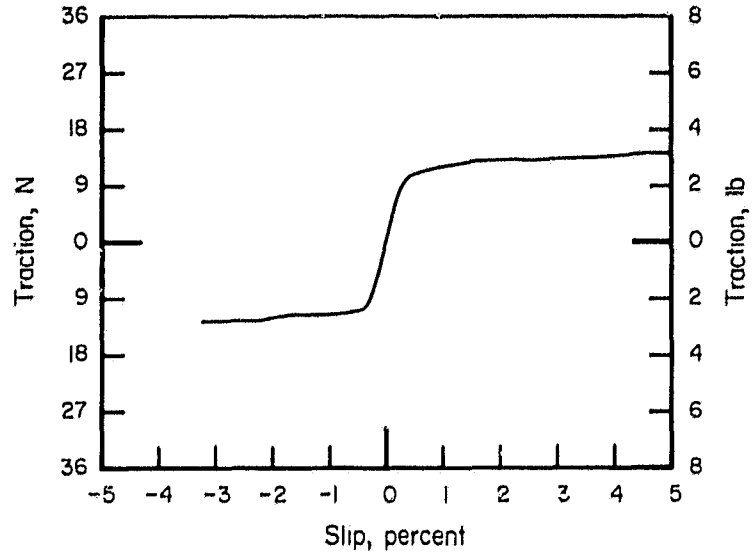

a. Disk contact pressure = 190 MPa (28 ksi)

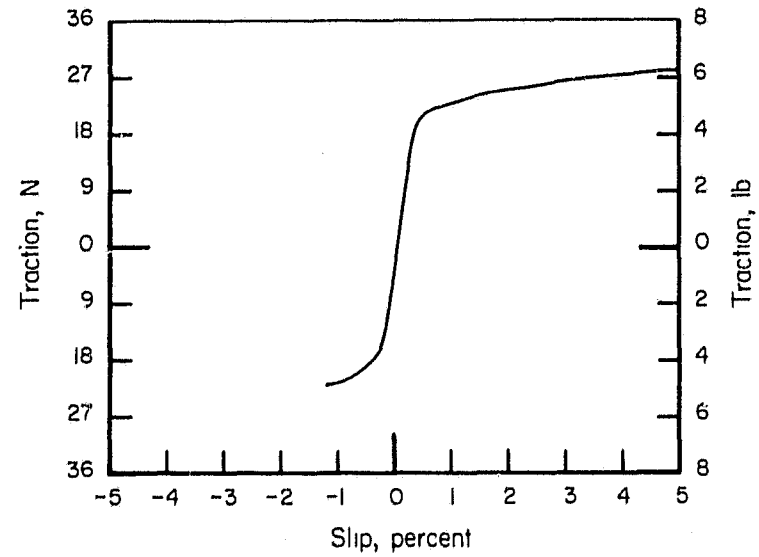

b. Disk contact pressure = 260 MPa (38 ksi)

FIGURE 7. SLIP-TRACTION CURVES FOR 76 mm (3.0 in.) DIAMETER DISK AT NOMINAL SPEED OF 5000 rpm

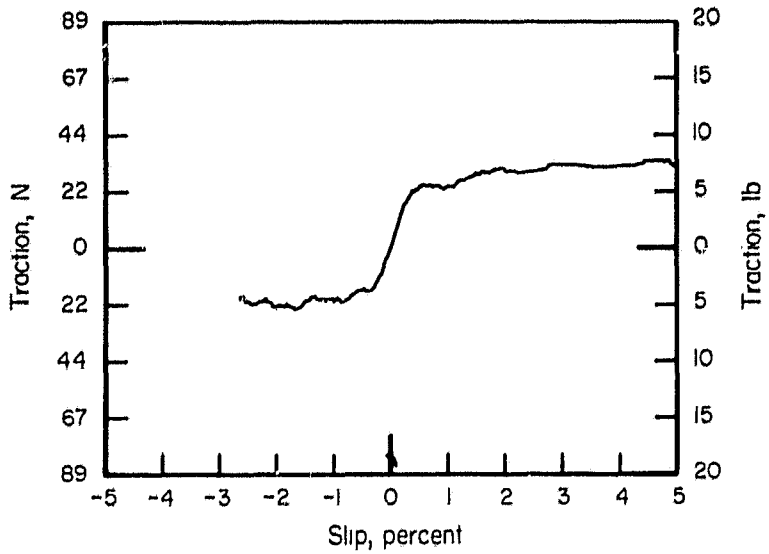

a. Disk contact pressure = 190 MPa (28 ksi)

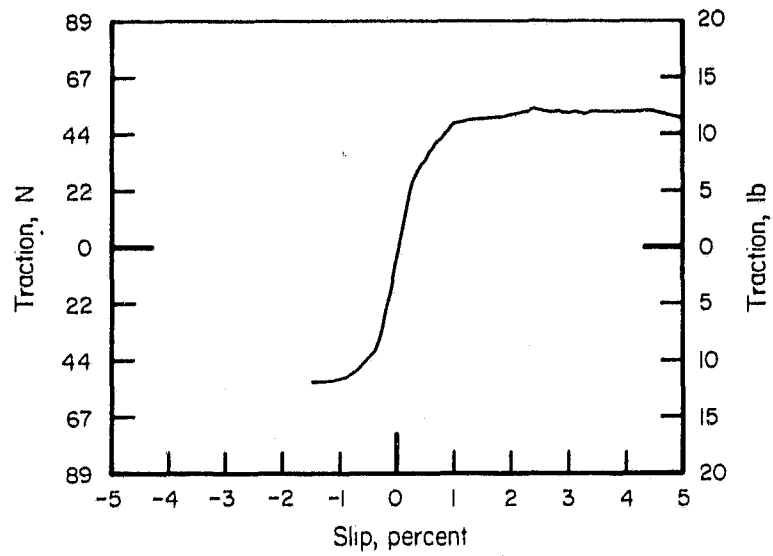

b. Disk contact pressure = 260 MPa (38 ksi)

FIGURE 8. SLIP-TRACTION CURVE FOR 76 mm (3.0 in.) DIAMETER DISK AT NOMINAL SPEED OF 10,000 rpm

TABLE 4. AVERAGE LN_2 VISCOSITY CALCULATED AS A FUNCTION OF PRESSURE

Contact Pressure, GPa (ksi)	Average Viscosity, (cp x 10^4)	
	At Disk Speed of 5000 rpm	At Disk Speed of 10,000 rpm
190 (28)	9	18
230 (33)	11	9
260 (38)	4	8
290 (42)	4	10

WEAR STUDIES ON AISI 440C STEEL

Apparatus and Procedure

The wear experiments were conducted on Battelle's high temperature 3-button apparatus, shown schematically in Figure 9. The upper disk specimen is mounted on a spindle, which provides the rotation and load through the head of the heavy duty drill press on which the apparatus is based. The three button specimens are mounted in a stainless steel cup, which serves to retain fluids and to be the receptor for an induction heating coil. The cup is mounted on a center ball for self-leveling of the three buttons and is coupled to a lower pedestal with a single pin. The lower pedestal is mounted on rolling element bearings and is restrained from motion by a load cell, which provides a continuous measurement of the dynamic torque. The friction is monitored continuously and recorded on a strip-chart. The button temperature is monitored with a thermocouple inserted through the cup and held in contact against the bottom of one of the buttons. The apparatus can apply total loads from 196 N (44 pounds) to 3560 N (800 pounds). Rotational speeds from 10 rpm to 3600 rpm are available, which correspond to 0.041 m/s (1.6 in./s) to 97 m/s (3800 in./s), respectively, at the 0.038 m (1.5 in.) radius of the button location.

The disks and buttons were prepared from AISI 440C stainless steel, which was heat treated in accordance with the procedures used on the actual bearing components for the HPOTP. The final hardnesses were HRC 58-60. The buttons were 7.94 mm (0.3125 in.) in diameter. Both the disks and buttons were finished by grinding to a surface finish of 0.23 μm (9 μin.) average roughness.

An initial run proved to be too severe at a rotational speed of 850 rpm, which corresponds to a sliding speed of 3.38 m/s (133 in./s) and a load of 890 N (200 pounds), or 18 MPa (2600 psi). Subsequent tests were run at rotational speeds of 180 rpm, which corresponds to a sliding speed of 0.718 m/s (28.3 in./s). The total load on the three button ranged from 196 N (44 pounds) to 520 N (117 pounds), or 3.9 MPa (570 psi)

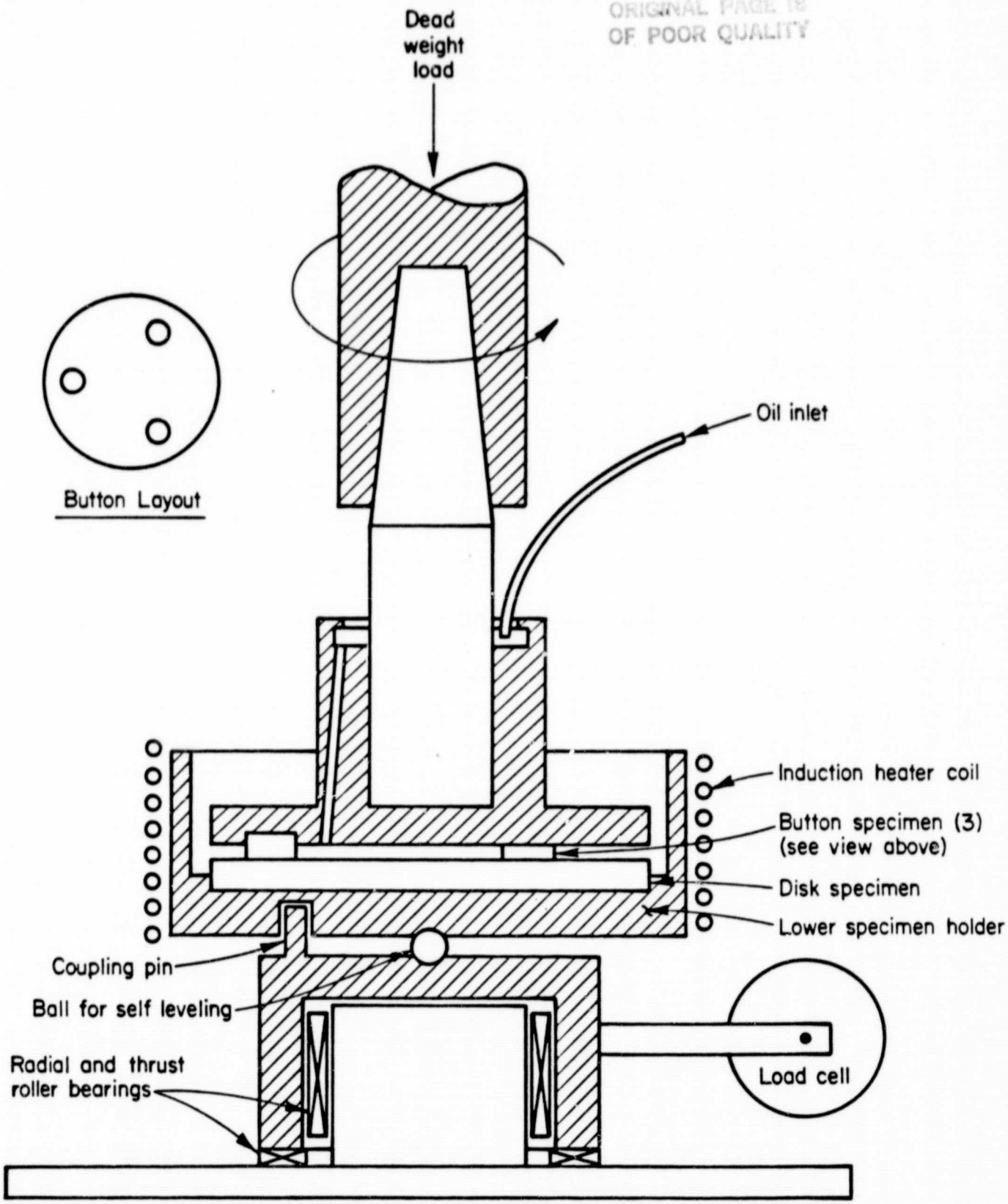

FIGURE 9. HIGH TEMPERATURE 3-BUTTON FRICTION AND WEAR APPARATUS

to 10.5 MPa (1530 psi), respectively. The maximum was established experimentally to be the highest allowable for avoiding a severe wear regime. The typical running times were 60 minutes unless severe wear or temperature control problems required a reduction.

Wear Results

The results of the wear experiments are presented in Table 5. The running conditions for Experiment 1, 18,000 Pa (2600 psi contact pressure and 3.4 m/s [133 in./s]), proved to be very aggressive in that 0.74 mm (0.029 in.) of wear occurred on the buttons in 7 seconds. More reasonable rates were measured with the sliding velocity decreased to 0.70 m/s (28.3 in./s) and the loads reduced. The coefficients of friction were generally high, with the highest observed in the intermediate temperature range from room temperature to 320 C (600 F).

The Archard wear equation was used to evaluate the results of the experiments and permit a comparison of the wear coefficients.

$$V = \frac{k\,L\,x}{3\,p} \quad , \tag{4}$$

where

V = wear volume
k = wear coefficient
L = applied load
x = sliding distance
p = hardness.

With data from measurements of the actual hardnesses at the running temperatures (described in a later section of this report), the wear coefficients were calculated for the experiments, Table 5. The graphical presentation in Figure 10 shows an increase in the wear coefficients in the intermediate temperature range. The liquid nitrogen environment for the low-temperature test may promote a lower coefficient by maintaining the full hardness on a local basis, whereas the frictional heating could cause local softening in the intermediate temperature range. At the elevated temperatures, a distinct continuous blue oxide film was present

TABLE 5. RESULTS OF THREE-BUTTON WEAR EXPERIMENTS ON SELF-MATED AISI 440 C

Experiment Number	Total Load, N (lb)	Contact Pressure, kPa (ksi)	Sliding Speed, m/s (ft/s)	Temperature, C (F)	Running Time, minutes	Coefficient of Friction	Average Button Wear, mm (in.)	Button Wear Wear Coefficient, x 10^{-5}
1	890 (200)	18 (2.6)	3.4 (11)	21 (70)	0.12 (7 s)	0.7	0.74 (0.029)	8000
2	520 (117)	10 (1.5)	0.70 (2.3)	170 (330)	60	0.5	1.40 (0.055)	330
3	196 (44)	4 (0.6)	0.70 (2.3)	LN_2	60	0.3	0.005 (0.0002)	3.1
4	520 (117)	10 (1.5)	0.70 (2.3)	LN_2	60	0.4	0.018 (0.0007)	95
5	196 (44)	4 (0.6)	0.70 (2.3)	93 (200)	60	0.5	0.086 (0.0034)	53
6	196 (44)	4 (0.6)	0.70 (2.3)	320 (600)	40	0.7	0.267 (0.0105)	180
7	520 (117)	10 (1.5)	0.70 (2.3)	320 (600)	11	1.0	1.03 (0.0404)	970
8	196 (44)	4 (0.6)	0.70 (2.3)	650 (1200)	10	0.4	0.051 (0.0020)	120
9	520 (117)	10 (1.5)	0.70 (2.3)	650 (1200)	56	0.4	0.079 (0.0031)	12
10	520 (117)	10 (1.5)	0.70 (2.3)	760 (1400)	60	0.2	0.038 (0.0015)	4.6
11	520 (117)	10 (1.5)	0.70 (2.3)	320 (600)	60	0.5	0.457 (0.0180)	79
12	520 (117)	10 (1.5)	0.70 (2.3)	200 (390)	60	0.6	0.975 (0.0384)	230
13	520 (117)	10 (1.5)	0.70 (2.3)	650 (1200)	60	0.5	0.071 (0.0028)	10
14	356 (80)	7 (1.0)	0.70 (2.3)	LN_2	60	0.3	0.23 (0.0092)	79
15	520 (117)	10 (1.5)	0.70 (2.3)	LN_2	60	0.4	0.18 (0.0069)	41

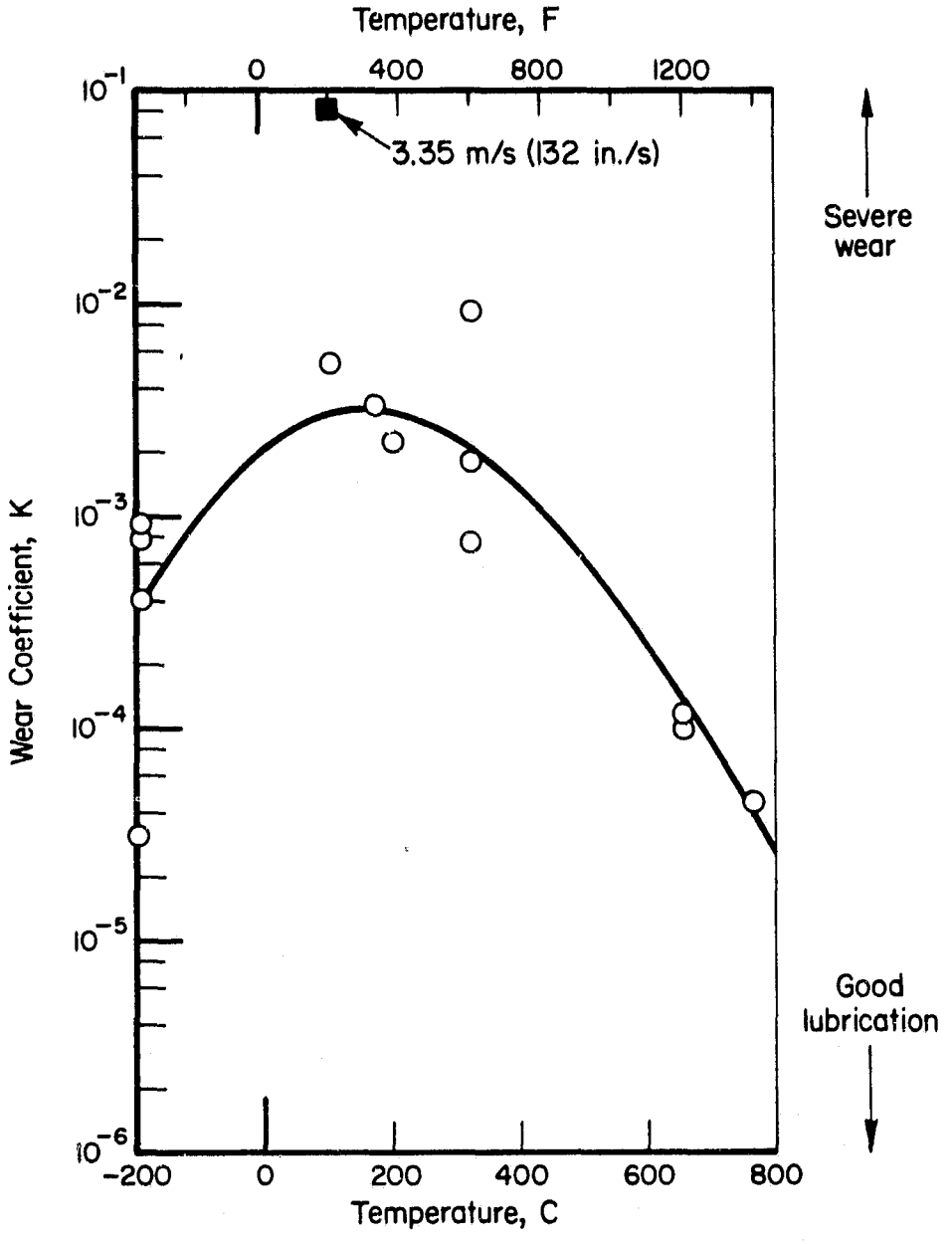

FIGURE 10. EFFECT OF TEMPERATURE ON WEAR COEFFICIENT OF AISI 440C BUTTONS

on the buttons and disk wear track, which apparantly served as a lubricant regardless of the low hardnesses. The Archard wear coefficient has been observed to range over several orders of magnitude in general engineering practice. As shown in Figure 10, most of the current wear coefficients fell in the intermediate range between severe wear and the very low wear rates associated with good (hydrodynamic) lubrication.

Application to HPOTP Bearings

The most severe wear problem of the HPOTP bearings has been with the balls. Diametral wear on the order of 0.2 mm (0.008 in.) has been observed, which occurs nearly uniformly on all of the balls of the complement. The wear has been observed in test engines and appears to occur in relatively short time intervals (on the order of a normal launch time of 800 seconds). With the wear data generated from the 3-button tests, a calculation was made of the expected amounts of wear on the HPOTP balls.

Previous analyses of the HPOTP-turbine-end bearings have shown that the average sliding velocity between the balls and races is approximately 0.81 m/s (32 in./s) at a 100 percent speed and a 3600 N (800 pounds) axial load[4]. The ball-race contact load under these conditions is approximately 800 N (180 pounds), which results in an average contact pressure of 670 MPa (100,000 psi). With these parameters and the ball hardness of HRC 60, a calculation can be made of the volume of ball wear as a function of operating time from Equation (4).

The expected diametral ball wear at three wear coefficients is shown in Figure 11. With a wear coefficient of 10^{-4} or lower, the predicted ball wear is minimal. Wear coefficients on the order of 10^{-5} to 10^{-7} are typical in sliding systems operating with excellent lubrication (hydrodynamic or complete solid lubricant films separating the metallic members). With a wear coefficient of 10^{-3}, diametral ball wear of 0.1 mm (0.004 in.) would be expected in a launch cycle of 800 seconds. Compared with the accuracy to which the balls are manufactured (roundness and matched ball sizes of 0.25 μm (0.00001 in.)

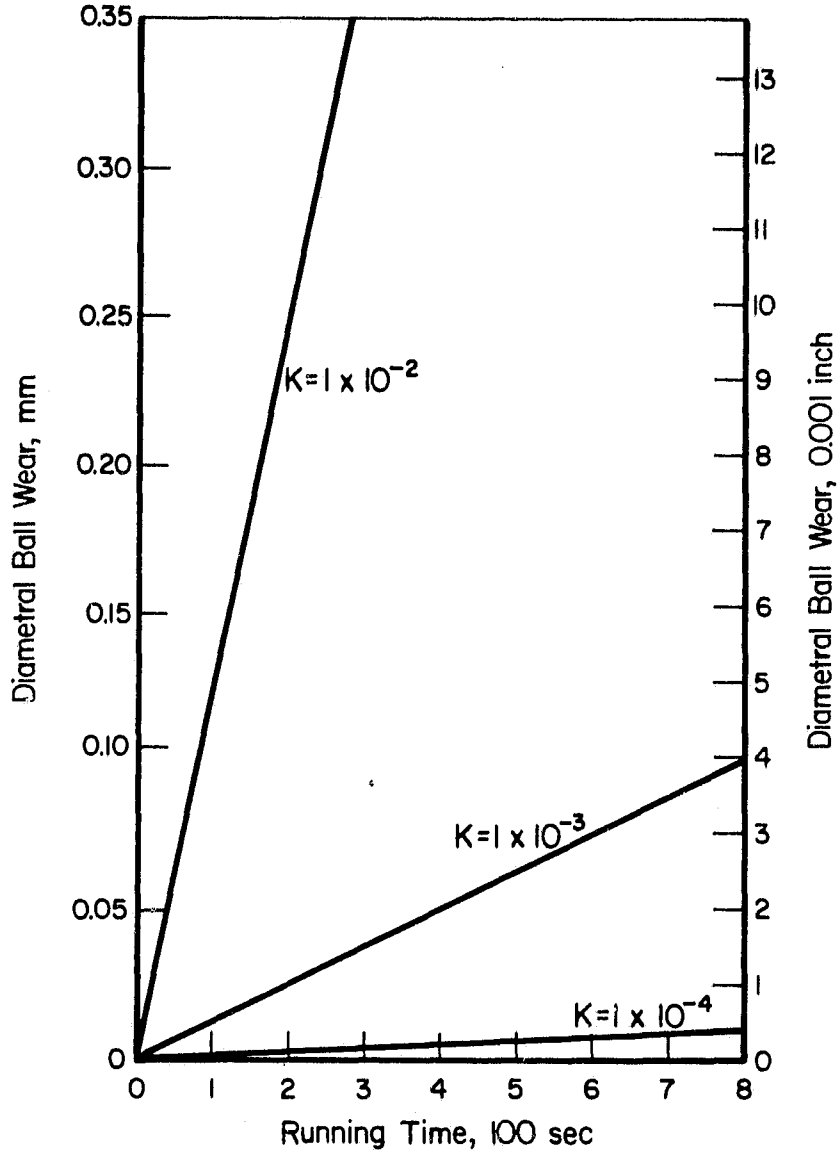

FIGURE 11. EXPECTED HPOTP BALL WEAR WITH THREE WEAR COEFFICIENTS AT A 3600 N (800 POUNDS) AXIAL LOAD

or less), wear of 0.1 μm (0.004 in.) completely destroys the original precision of the bearing. As the wear coefficient reaches 10^{-2} or greater, which was measured with the relatively modest contact pressures of the wear tests, the ball wear rate is sufficiently high to account for the observed ball wear in under 200 seconds of operation.

While the similitude between the HPOTP balls and the three-button wear tests is not good and the predictive capability of the Archard equation is only approximate, the results clearly show that good lubrication is required to avoid ball wear. The ball-race sliding velocity and loading are sufficiently high to cause significant ball wear in the absence of lubrication. The oxide films that caused the reduction in ball wear at the high temperatures (with the three-button tests) probably cannot be depended upon for lubrication in service because the associated material hardness would be inadequate to support the contact pressures (discussed in the following section of this report). Therefore, efforts should be continued to identify means for providing a dependable lubrication mechanism for the HPOTP bearings.

TEMPERING BEHAVIOR AND HOT HARDNESS OF AISI 440C

The high speed of the HPOTP shaft (approximately 30,000 rpm) and the poor lubricating properties of the liquid oxygen combine to generate large amounts of heat in the HPOTP bearings. Maintaining cryogenic temperatures at the bearings depends critically upon a continuous flow of liquid oxygen through the bearings. If the supply is temporarily interrupted or if high transient loads cause sufficient heat generation in the bearings to vaporize the oxygen, the danger exists of developing high bearing component temperatures over brief periods of time. Therefore, an experimental study was conducted to determine the short-term tempering behavior of the AISI 440C bearing steel to determine the times required at elevated temperatures to cause measurable reductions in hardness. A study was also made of the hot hardness to determine the actual hardness available at longer times at elevated temperatures.

Short-Term Tempering Behavior

Specimens

The specimens were AISI 440C rods 7.9 mm (0.313 in.) in diameter by 100 mm (4 in.) in length, which were heat treated to HRC 60 in accordance with the procedures specified for the HPOTP bearings. Following heat treating, they were centerless ground to 6.35 mm ($0.250\ ^{+0.002}_{-0.000}$ in.). Two flats measuring approximately 51 mm (2 in.) in length and 0.25 mm (0.010 in.) deep were ground at the center of each specimen and 180 degrees apart to permit hardness impressions on flat surfaces.

Experimental Procedure

The apparatus used for tempering the test specimens by resistance heating was a Duffers Gleeble Model 510 having a Model 766 function generator. Power for heating is supplied by an AC transformer and transmitted to the ends of the specimen through water-cooled cooper jaws spaced 19 mm (0.75 in.) apart. A chromel-alumel (Type K) thermocouple was percussion welded to each specimen at the midpoint between the jaws to provide a millivolt signal to the function generator for temperature control. The specimens were heated to the tempering temperature in 2 seconds, held at temperature for a predetermined amount of time, and allowed to cool by shutting the power off. The specimens cooled to 110 C (200 F) below each tempering temperature in approximately 3.5 seconds.

Results

A plot of hardness versus time at the tempering temperature is shown in Figure 12. Tempering at 540 C (1000 F) for 10, 105, and 945 seconds reduced the hardness from the initial value of HRC 60 to HRC 57-58. This indicates that a small reduction of hardness occurs

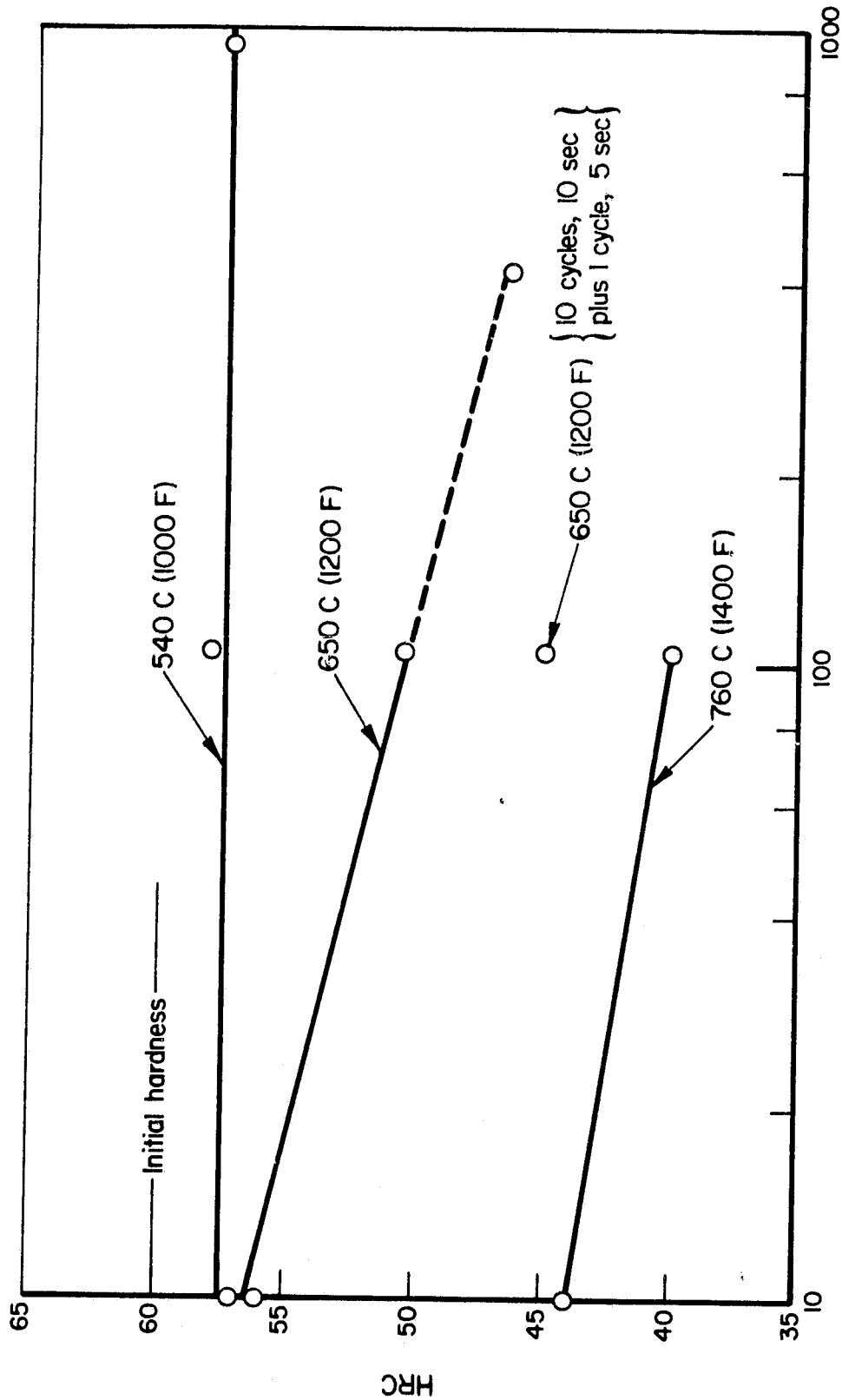

FIGURE 12. EFFECT OF TEMPERING TIME AND TEMPERATURE ON THE HARDNESS OF AISI 440 C

during tempering at 540 C (1000 F), but softening did not increase with time between 10 and 945 seconds. Tempering at 650 C (1200 F) for 10 seconds reduced the hardness about as much as tempering at 540 C (1000 F) for 10 seconds. However, with increasing time (105 and 420 seconds) the hardness was reduced to HRC 50.5 and HRC 46.5, respectively. At 760 C (1400 F) the hardness was reduced to HRC 44 in 10 seconds and HRC 40 in 105 seconds. Also plotted on Figure 12 is the hardness of a specimen heated 10 times to 650 C (1200 F) and held at temperature for 10 seconds and heated once to 650 C (1200 F) and held at temperature for 5 seconds. The hardness, HRC 45, is lower than that of a specimen heated once to 650 C (1200 F) and held at the tempering temperature for 105 seconds, HRC 50.5. The lower hardness probably resulted from tempering that occurred during heating (3.92 total seconds above 540 C [1000 F]) and cooling (38.5 total seconds above 540 C [1000 F]).

All of the data can be plotted on a single curve as shown in Figure 13[5]. The empirical tempering parameter includes absolute temperature, an empirically developed constant, and the logarithm of the time at temperature in seconds. The relationship was developed from time-and-temperature tempering data for a variety of low-alloy steels having a range of carbon contents. Although the alloy content of AISI 440C is different from any of the alloys evaluated in the study, most of the data conform to the expected linear relationship for parameter values greater than 25,000. The two points below 25,000 resulted from the 10 second and 100 second tempering times at 540 C (1000 F), both of which were well below the times considered in the studies on which the parameter is based. The plot in Figure 13 is useful in predicting the expected hardness with other combinations of tempering time and temperature.

The microstructure of the as-heat-treated material (HRC 60) and after tempering for 105 s at 540, 650, and 760 C (1000, 1200, and 1400 F, respectively) are shown in Figure 14. Tempering produced only slight changes in the microstructure; the martensite appeared to coarsen and there was an apparant growth in the size and number of larger primary carbides.

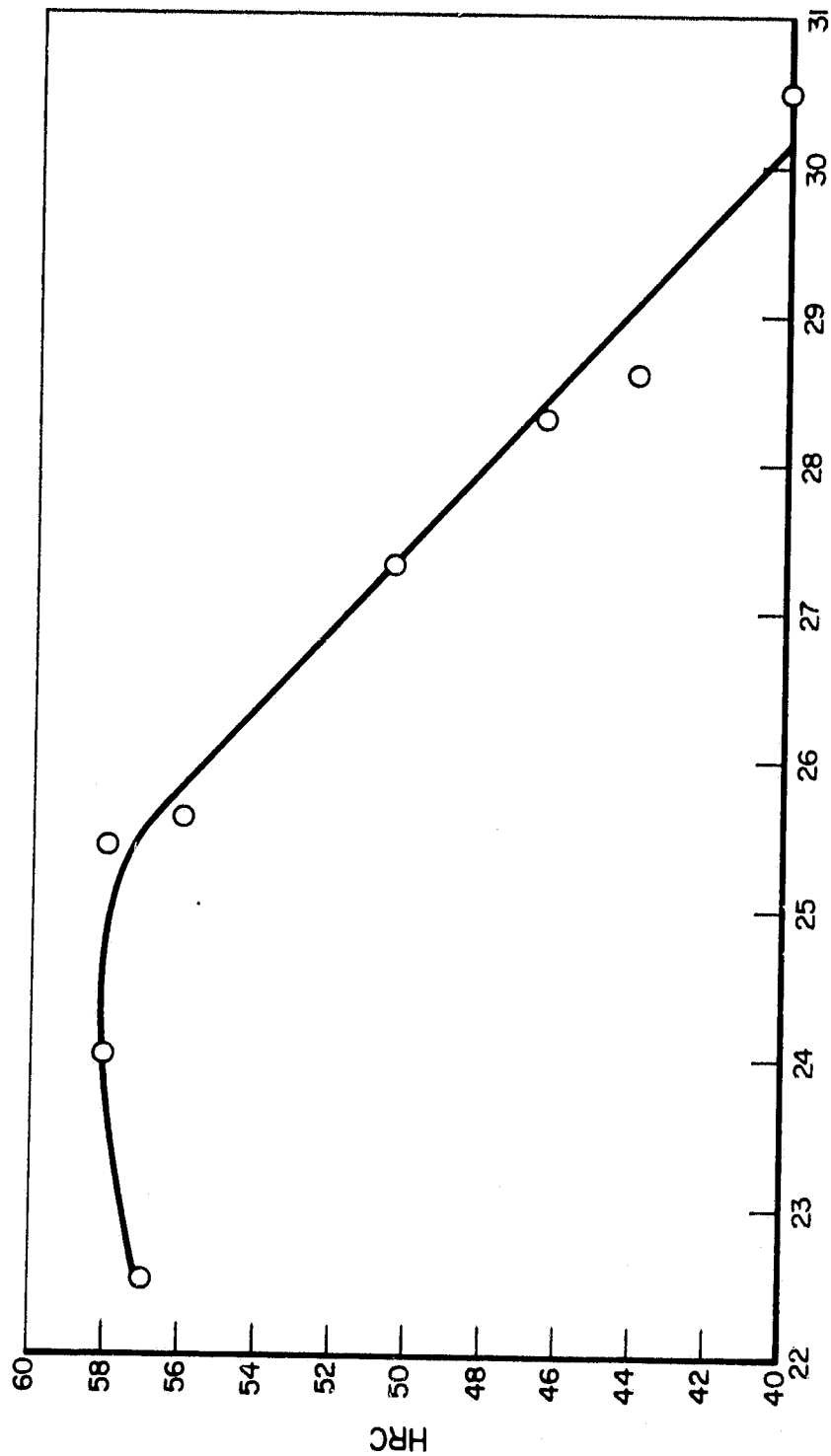

FIGURE 13. HARDNESS OF TEMPERED AISI 440 C AS A FUNCTION OF AN EMPERICAL TIME-TEMPERATURE PARAMETER

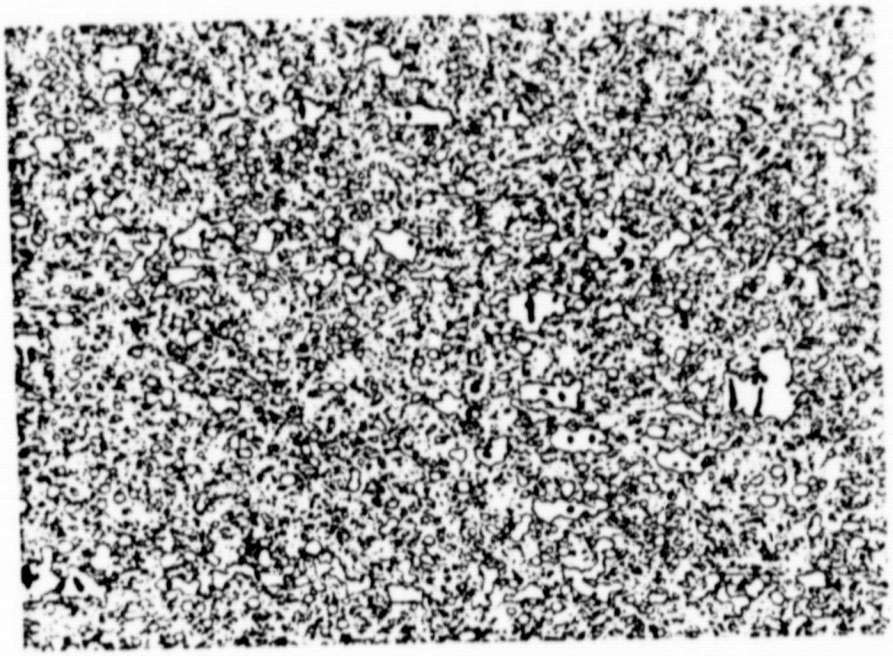

750X 4L611

a. As heat treated to HRC 60

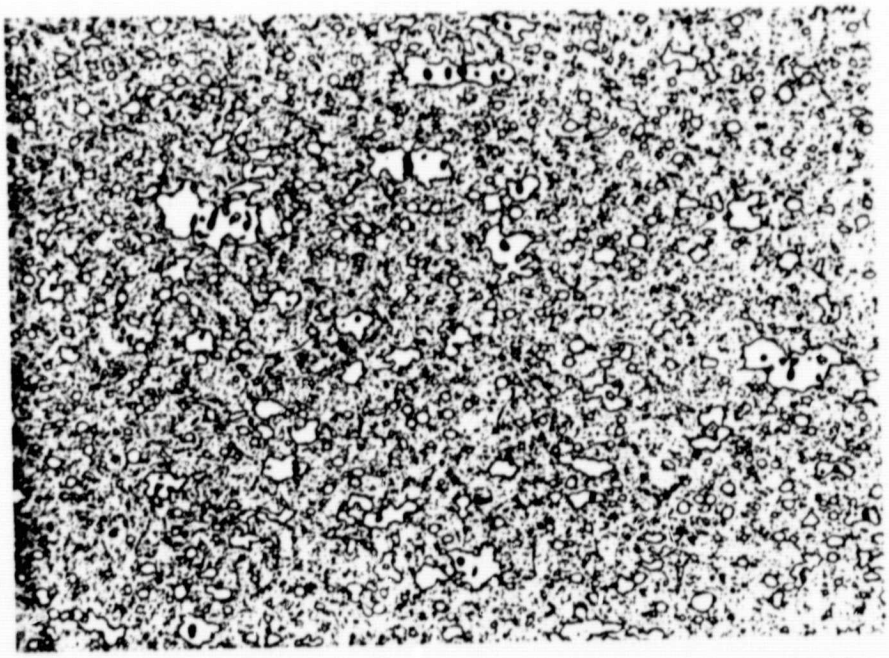

750X 4L612

b. After tempering at 540 C (1000 F) for 105 s, HRC 58

FIGURE 14. EFFECT OF TEMPERING ON MICROSTRUCTURE OF AISI 440 C

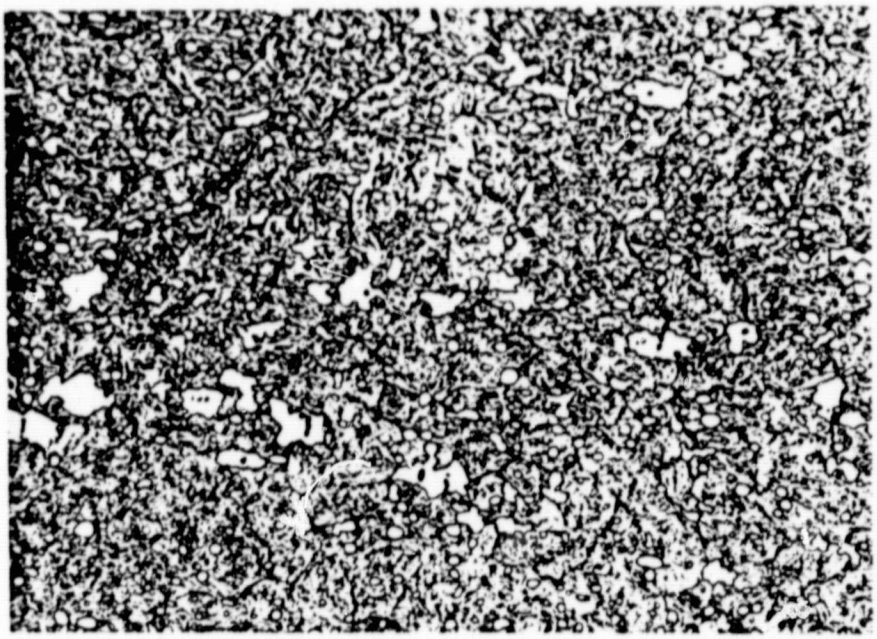

750X 4L614

c. After tempering at 650 C (1200 F) for 105 s, HRC 51

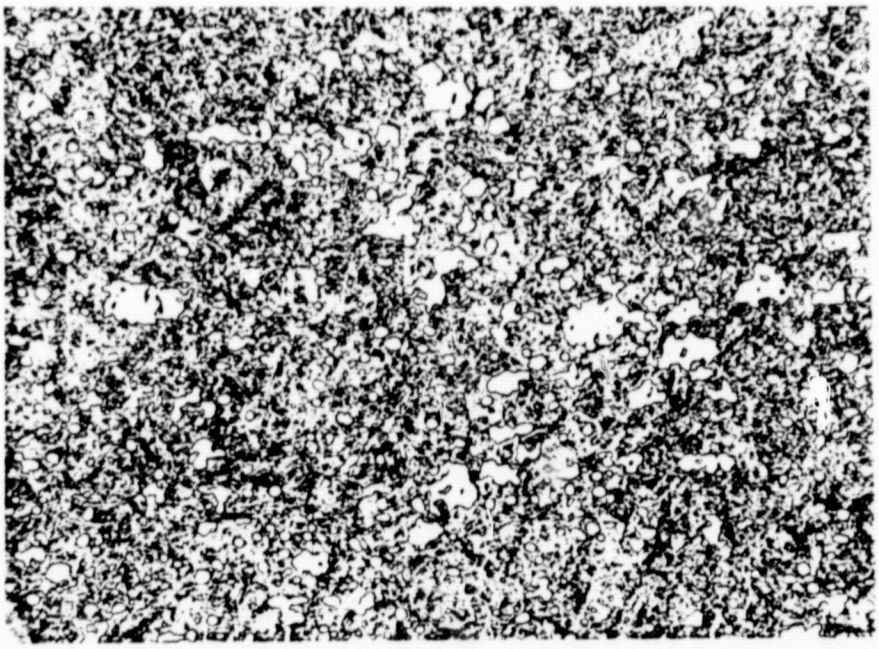

750X 4L613

d. After tempering at 760 C (1400 F) for 105 s, HRC 58

FIGURE 14. (Continued)

Hot-Hardness Measurements

The hot-hardness measurements were made on samples of AISI 440C cut from an acutal used HPOTP bearing race, which measured HRC 60 at room temperature. Three specimens were placed in the hot-hardness apparatus, which heats the specimens in a vacuum to the desired temperature, and loads applied to a diamond indentor for obtaining diamond pyramid hardness numbers (DPHN). The hardness impressions were made successively at different locations on the specimen as the temperature was increased in steps from 540 C (1000 F) to 820 C (1500 F). The sizes of the impressions were measured after the test at room temperature to obtain the DPHN values.

A plot of the measured hot hardnesses on the three specimens is presented in Figure 15. The hot hardness was seen to decrease very rapidly with temperatures of 540 C (1000 F) and above. The hardness of less than DPHN 300 (HRC 30) at 540 C (1000 F) was well below the hardness values required for pratical service of rolling element bearings. Therefore, bulk temperatures of 480 C (900 F) or greater could not be tolerated from the standpoint of resulting hardness in the HPOTP bearings.

MEASURING AND CALCULATING UNITS

Since the bearing drawings and all input data provided by NASA were in English units, all measurements and calculations were performed in English units. The SI units presented in this report were converted from English units. The data on which the report is based are located in Battelle Laboratory Record Book 39381.

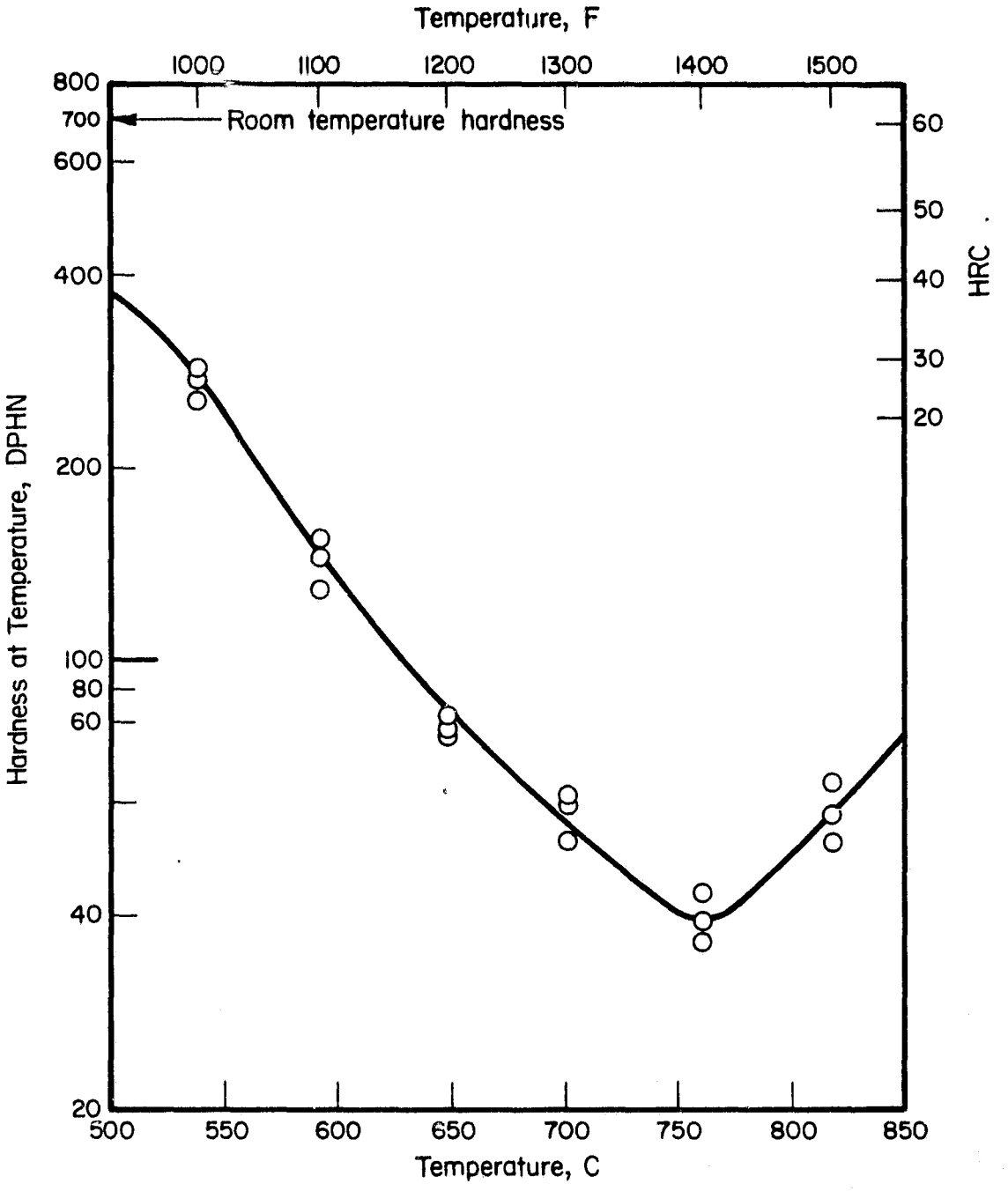

FIGURE 15. EFFECT OF TEMPERATURE ON HOT HARDNESS OF AISI 440 C

REFERENCES

1. Grubin, A. N., and Vinogradova, I. E., "Investigation of the Contact of Machine Components", Moscow, TsNIITMASh, Book No. 30, (1949), (D.S.I.R., London, Translation No. 337).

2. Bell, J. C., "Lubrication of Rolling Surfaces by a Ree-Eyring Fluid", A.S.L.E. Paper at the Lubrication Conference, Chicago, Illinois, October, 1961.

3. Timoshenko, S., Strength of Materials, 2nd Edition, D. Van Nostrand Co., New York, (1940), pp 555-560.

4. Kannel, J. W., Merriman, T. L., Stockwell, R. D., and Dufrane, K. F., "Evaluation of Outer Race Tilt and Lubrication on Ball Wear and SSME Bearing Life Reductions", Final Report to NASA/Marshall Space Flight Center, July 7, 1983.

5. Grange, R. A., and Baughmann, R. W., "Hardness of Tempered Martensite in Carbon and Low-Alloy Steel", Transactions ASM, Vol 48, pp 165-197, (1956).